Atomic and electronic structures of α-Al_2O_3 surfaces

Takahiro Kurita,* Kazuyuki Uchida, and Atsushi Oshiyama†
Department of Applied Physics, The University of Tokyo, Hongo, Tokyo 113-8656, Japan
and CREST, Japan Science and Technology Agency, Sanbancho, Tokyo 102-0075, Japan
(Received 2 June 2010; revised manuscript received 22 September 2010; published 21 October 2010)

We present the first-principles total-energy electronic-structure calculations that provide a firm theoretical framework to consider atomic and electronic structures of alumina surfaces. Exploring detailed atomic structures and electron states of stable and metastable surfaces of three important planes, C plane [the (0001) surface], R plane [the $(1\bar{1}02)$ surface], and A plane [the $(11\bar{2}0)$ surface], of α-Al_2O_3, we find that the stoichiometric surface of the C plane has the lowest surface energy, followed by the stoichiometric surfaces of the R plane and then the A plane, irrespective of the chemical potentials of constituting elements. Detailed atomic structures for stable and metastable surfaces of each plane have been obtained, which is imperative for atom-scale clarification of reactions on the α-Al_2O_3 surface. The electron states of each surface have been calculated in detail. The obtained surface energy bands offer a possibility to identify atomic structures of α-Al_2O_3 surface by spectroscopic measurements. It is found that the ionic interaction between Al and O and the covalent interaction among Al atoms or O atoms are both important to determine the surface atomic structures.

DOI: 10.1103/PhysRevB.82.155319 PACS number(s): 68.35.Md, 73.20.At, 68.35.bg

I. INTRODUCTION

Alumina, i.e., aluminum oxide with chemical formula Al_2O_3, known for its doped brilliant forms sapphire and ruby, is an important material at various stages in technology. It is the raw material for aluminum production, used as abrasive and cutting tools, a good coating material for mechanical and anticorrosive protection, and a supporting material for catalytic reactions. This high utility comes from its hardness and stability against harsh environments. It is also a typical metal oxide and offers a good stage where roles of metallicity, ionicity, and possible covalency in material properties are clarified.

Alumina has several polymorphs and α-Al_2O_3 occasionally called corundum is the most stable crystalline form. In microelectronics and nanoelectronics, α-Al_2O_3 is used as a dielectric and also widely employed as a substrate for other active materials. Nitride semiconductors are epitaxially grown on α-Al_2O_3,[1,2] and recently carbon nanotubes are aligned, in particular, directions of its certain surfaces.[3–5] Microscopic identification of atomic and electronic structures of α-Al_2O_3 surfaces thus becomes imperative in applications in current technology. Scientifically, surfaces of metal oxides have been less pursued[6] than semiconductor surfaces, and clarification of underlying physics and chemistry of α-Al_2O_3 surfaces is of interest.

α-Al_2O_3 crystallizes in a structure which is described by a primitive rhombohedral unit cell or by a conventional hexagonal unit cell [Fig. 1(a)]. In the hexagonal unit cell, the atoms are stacked along the [0001] direction in a sequence of Al double layers and an oxygen layer: i.e., -$AlAlO_3AlAlO_3$- [Fig. 1(b)]. The oxygen atoms form a hexagonal close-packed structure and the aluminum atoms are located at two thirds of octahedral sites of the oxygen sublattice. Consequently, the coordination number of oxygen is 4, whereas it is 6 for aluminum. The most common surface is the (0001) surface called C plane. Other surfaces such as the $(1\bar{1}02)$ surface and $(11\bar{2}0)$ surface, called R plane and A plane, respectively, are also employed in the application: Carbon nanotubes are indeed aligned along particular directions of R plane and A plane.[3–5] Compared to monatomic materials, determining the surface structure of the compound α-Al_2O_3 is accompanied with certain complexity. Even when we are restricted to the ideal (unrelaxed) C plane, there are three distinctive ways of termination to form the surface. Termination at a single Al layers (Al-I surface), at an O layer (O-I surface), and at an Al double layer (Al-II surface) generates three inequivalent surfaces [Fig. 1(b)]. Furthermore these three surfaces have different stoichiometries near the surface.

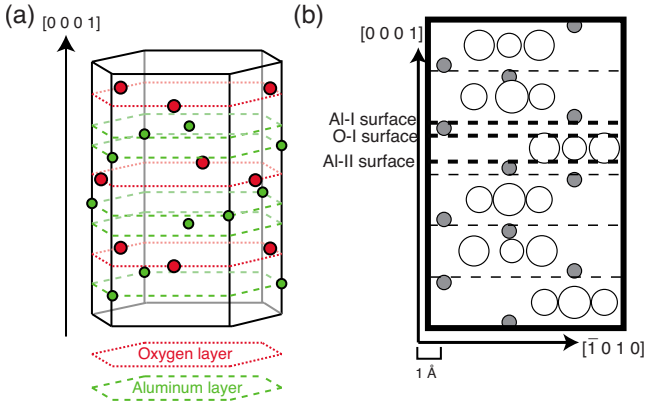

FIG. 1. (Color online) (a) Atomic structure of α-Al_2O_3 (corundum). Large red and small green circles depict oxygen and aluminum atoms, respectively. Oxygen atoms are at midpoints of sides, and aluminum atoms are at vertices or center of hexagonal lateral unit cell. (b) Illustration of the 12 Al layers and 6 O layers of α-Al_2O_3 in hexagonal unit cell. Three distinctive surfaces labeled as Al-I, O-I, and Al-II of the C plane [(0001) plane] are shown by thick dashed lines. The thin dashed lines show a basic AlO_3Al layer unit. Large white and small gray circles depict oxygen and aluminum atoms, respectively.

Therefore their surface energies depend differently on the oxygen and aluminum chemical potentials.

Most works for α-Al_2O_3 surface in the past have been done for the C plane. The (0001) surface shows 1×1 lateral periodicity which is stable below 1100 °C. Above this temperature, oxygen partly evaporates[7] and the surface shows several reconstructions: $\sqrt{3}\times\sqrt{3}$ rotated by 30° at first, then $2\sqrt{3}\times2\sqrt{3}$ rotated by 30° at 1150 °C, $3\sqrt{3}\times3\sqrt{3}$ rotated by 30° at 1250 °C, and finally $\sqrt{31}\times\sqrt{31}$ rotated by 9° at 1350 °C.[7–9] The recent atomic force microscopy combined with the density-functional theory (DFT) calculations has shown that the $\sqrt{31}\times\sqrt{31}R9°$ consists of Al adlayers on the Al_2O_3 substrate.[10]

As for the most stable 1×1 structure, from x-ray diffraction[11] and ion-scattering[12,13] experiments, it is argued that the surface is Al-I terminated. On the other hand, a low-energy electron diffraction (LEED) data[14] is best explained by an assumption that the surface is a mixture of Al- and O-terminated domains with a ratio of 2:1. However, another LEED experiment[15] shows after examining various domain structures that the surface is Al-I terminated.

Theoretical calculations for Al_2O_3 surface have been performed mainly for the Al-I surface of the C plane.[16–29] The calculation methods range among a tight-binding model,[19] the local-density discrete-variational method,[17] the Hartree-Fock,[16,21] the local-density,[25] and the generalized-gradient[26,27] approximations (GGA) as implemented in the code CRYSTAL, the Gaussian-based pseudopotential method in the DFT,[22] the plane-wave pseudopotential DFT method,[18,20,23,28,29] and the full-potential linearized augmented plane-wave method.[24] Models and methods adopted in these calculations are different and thus the quantitative accuracy of the obtained results is diverse. One of the characteristic features in the calculated results, however, is that large relaxation of the topmost Al layer to the second oxygen layer. Calculated amount of the relaxation, compared with the layer-layer distance in the unrelaxed structure, is 48% in the HF calculation[16] and 86% and 87% in the DFT calculations.[18,22,24] Experiments found the first-layer contraction being about 35% and the discrepancy between the calculations and the experiments are discussed in terms of anomalous thermal vibrations[15] or hydrogen adsorption.[24] As for electron states, surface energy bands for the Al-I surface of the C plane is only available from the tight-binding calculation,[19] and the origin of the experimentally believed insulating behavior of the C plane is unclear.

Adsorption of Al and O elements[30,31] and of other metallic elements[31] on the Al-I surface of the C plane has been examined by the DFT calculations. The adsorption of metallic elements are generally important for microscopic identification of catalytic reactions, and the Al and O adsorption is related to clarifying stability of other surfaces of the C plane. For instance, surface energies of Al-rich surfaces, including Al-II surface, are found to be higher than that of the Al-I surface (occasionally called stoichiometric surface) and the H covered O-I surface is the most stable in O-rich environments.[23,24] For ultrathin aluminum oxide on NiAl(110) substrate, a peculiar oxygen-deficient line defects have been identified by scanning tunneling microscopy combined with DFT calculations.[32,33] Knowledge on detailed electronic structures of the nonstoichiometric surfaces of the C plane are lacking, however.

Knowledge about atomic and electronic structures of the R plane [$(1\bar{1}02)$ surface] and the A plane [$(11\bar{2}0)$ surface] is relatively poor, although they are technologically as important as the C plane. LEED (Ref. 34) and crystal rod truncation diffraction (CRTD) (Ref. 35) experiments have been performed for the R plane. There are five ways of termination for the unrelaxed R plane, as will be explained in the following section. The CRTD data were examined by considering two of the five termination possibilities and an oxygen-terminated surface was proposed for the R plane.[35] The surface energy for one possible termination was calculated by three different groups[20,29,36] and the results from the two groups agree within 4% discrepancy.[20,29] As for the A plane, electronic microscopy,[37] LEED,[38] He-atom scattering[39] experiments have been performed. It is found that the 1×1 structure is stable, although 12×4 superstructure is observed at temperature higher than 1400 °C. The surface energy for one possible termination was calculated by two different groups[20,29] and the results differ from each other by 23%. At present stage, energetics among differently terminated surfaces, detailed atomic arrangements for each surface after relaxation, and their electronic structures of the R and the A planes are unknown yet.

In this paper, we report total-energy electronic-structure calculations based on the density-functional theory which provide detailed atomic structures, surface stoichiometries (i.e., energetically favorable terminating ways to generate surfaces), energetics for various surfaces as a function of chemical potentials of constituting elements, and furthermore electronic structures of stable and metastable surfaces of the C, R, and A planes of α-Al_2O_3 on an equal theoretical footing. The organization of this paper is as follows. In Sec. II, a brief description of our DFT calculations is given. Some details to assure accuracy of surface energies within several millielectron volts per square angstroms are described. Our results for atomic structures and electron states for the C, R, and A planes of α-Al_2O_3 are presented in Sec. III. Section IV summarizes our findings.

II. CALCULATIONS

Total-energy electronic-structure calculations in the present paper have been performed in the DFT (Refs. 40 and 41) with the GGA proposed by Perdew, Burke, and Ernzerhof[42] for exchange-correlation energy functional. Nuclei and core electrons are simulated by ionic pseudopotentials generated in the GGA. For an Al ion, we generate norm-conserving pseudopotentials[43,44] following the recipe by Troullier and Martins.[45] For an O ion, we generate ultrasoft pseudopotentials by Vanderbilt.[46] Kohn-Sham equations[47] are solved self-consistently by introducing plane-wave basis sets. In the optimized geometries, all the atomic coordinates are optimized according to the calculated Hellmann-Feynman forces. In the optimized geometries, the forces acting on atoms are less than 5×10^{-2} eV/Å in this paper. Computations have been performed using Tokyo *ab initio* program package (TAPP),[48–51] and pertinent features are ex-

TABLE I. Calculated structural parameters and heat of formation of α-Al_2O_3 along with the corresponding experimental values.

	a_R (Å)	α_R	u	v	ΔH (eV)
Calc.	5.17	55°26′	0.352	0.556	15.3
Expt.	5.128	55°20′	0.352	0.556	17.2

plained below. We regard 2*s* and 2*p* of O and 3*s* and 3*p* of Al as valence orbitals. We then examine transferability of the pseudopotentials used in the present work by changing their hardness and computing structural properties of Al metal and the O_2 molecule. We have changed the core radii between 1.1 bohr (1 bohr=0.0529 nm) and 1.5 bohr for O 2*s* and 2*p* orbitals, and then compute the bond length and the force constants of the O_2 molecule with the cutoff energy being in the range from 9 to 64 Ryd. We have found that the core radius of 1.3 bohr for both 2*s* and 2*p* orbitals combined with the cutoff energy of 36 Ryd for the plane-wave basis set is suitable to obtain the bond length within +1.2% deviation and the force constant within −3.3% deviation from the corresponding experimental values. It is noteworthy that this pseudopotentials also provide reliable results for water molecules in carbon nanotubes.[52] As for Al, we have changed the core radii between 1.6 and 2.0 bohr for 3*s* and 3*p* orbitals, and then compute the lattice constant and the bulk modulus of the face-centered-cubic Al with the cutoff energy being in the range from 9 to 64 Ryd. We have found that the core radius of 1.8 bohr for both 3*s* and 3*p* orbitals combined with the cutoff energy of 25 Ryd provides the lattice constant within −0.25% deviation and the bulk modulus within −2.9% deviation from the corresponding experimental values.

We thus use the pseudopotentials generated with the core radius of 1.3 bohr for O and 1.8 bohr for Al. The cutoff energy for the plane-wave basis set is set to be 36 Ryd in the present work. Using these calculation parameters, we next examine structural properties of α-Al_2O_3. The unit cell of α-Al_2O_3 is the rhombohedral containing two Al_2O_3 molecular units. There are four structural parameters: the side of the rhombohedral cell a_R, the angle α_R, and two internal parameters u and v. The calculated four parameters along with the experimental values are listed in Table I. The difference are +0.8% in a_R and +0.2% in α_R, respectively. The calculated values u and v agree with the experimental values to the third decimal place. We have also calculated heat of formation defined by

$$\Delta H = E_{Al_2O_3} - (2\mu_{Al}^{metal} + 3\mu_O^{O_2}), \tag{1}$$

where $E_{Al_2O_3}$, μ_{Al}^{metal}, and $\mu_O^{O_2}$ are the total energy per Al_2O_3 unit of α-Al_2O_3, the Al chemical potential in Al metal and the O chemical potential of an oxygen molecule, respectively. The calculated heat of formation is 15.3 eV which is in good agreement with the experimental value of 17.2 eV. Electronic energy bands are also calculated, and the results show that α-Al_2O_3 has a direct gap at the center of the Brillouin zone (BZ). The calculated energy gap is 6.1 eV which is a typical DFT underestimate of the experimental value of 8.8 eV.[53]

Surfaces are simulated by a repeating slab model in which an atomic slab consisting of sufficiently thick atomic layers is arranged periodically in the direction perpendicular to the layers with sufficiently thick vacuum regions between the slabs. α-Al_2O_3 has inversion symmetry so that we can prepare the slab with two equivalent top and bottom surfaces. Thicknesses of the slab and the vacuum region are crucial parameters which determine the accuracy of the calculated surface energies. We varies the thicknesses in the range between 10 and 20 Å. We have found that the slab thicknesses of 13.1 Å, 14.0 Å and 14.3 Å, for the C plane, the R plane, and the A plane, respectively, along with the 12-Å-thick vacuum region are enough to assure the convergence of the surface energy within several meV per $Å^2(5\times10^{-2}$ J/m^2). All the atoms in the slab are fully relaxed and it has been found that the atoms in the central layer of the slab are dislodged from the unrelaxed positions only by less than 0.1 Å.

The surface energy is the energy cost to form the surface and thus defined by

$$E_s = E_t - (n_{Al}\mu_{Al} + n_O\mu_O), \tag{2}$$

where E_t is the total energy of the slab system, n_{Al} and n_O are the number of Al and O atoms in the slab, and μ_{Al} and μ_O the chemical potentials of Al and O. Chemical potentials of aluminum and oxygen satisfy

$$E_{Al_2O_3} = 2\mu_{Al} + 3\mu_O, \tag{3}$$

where $E_{Al_2O_3}$ is the total energy per Al_2O_3 unit of α-Al_2O_3. Although chemical potentials vary depending on experimental environments, there are upper and lower limits. The upper limit of μ_O is the chemical potential of an oxygen molecule $\mu_O^{O_2}$ since μ_O larger than this value results in vaporization of oxygen as molecules from the Al_2O_3 surface. We call this environment as O-rich environment: i.e., $\mu_O^{O\ rich} = \mu_O^{O_2}$. In the O-rich environment, the Al chemical potential is given by

$$\mu_{Al}^{O\ rich} = \frac{E_{Al_2O_3} - 3\mu_O^{O\ rich}}{2}. \tag{4}$$

The lower limit of μ_O corresponds to the upper limit of μ_{Al} which is the Al chemical potential in Al metal μ_{Al}^{metal} since the larger μ_{Al} than this value results in segregation of Al metal from α-Al_2O_3. We call this environment as Al-rich environment: i.e., $\mu_{Al}^{Al\ rich} = \mu_{Al}^{metal}$. We have performed independent DFT-GGA calculations with same accuracy for O_2 molecules and face-centered-cubic Al metal, and obtained the necessary chemical potentials. It is found that $\mu_O^{Al\ rich}$ is lower than $\mu_O^{O\ rich}$ by 5.1 eV in the present calculation.

Using Eqs. (2)–(4) and the surface energy in the O-rich environment $E_s^{O\ rich}$, we may write the surface energy,

$$E_s = E_s^{O\ rich} - \frac{2n_O - 3n_{Al}}{2}(\mu_O - \mu_O^{O\ rich}), \tag{5}$$

as a linear function of the oxygen chemical potential.

In the experimental situation in which specimens are in equilibrium with vapor phases, the chemical potential can be expressed in terms of vapor pressure P and temperature T:

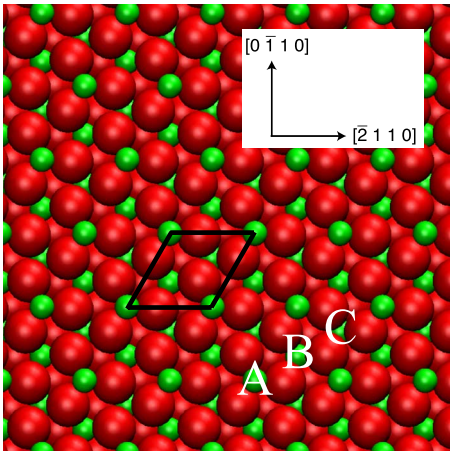

FIG. 2. (Color online) Top view of the unrelaxed Al-I surface of the C plane of α-Al_2O_3. Large red and small green balls depict oxygen and aluminum atoms, respectively. The solid-line parallelogram indicates 1×1 lateral unit of the C plane. Labels A, B, and C indicate three Al sites (see text).

i.e., $\mu_O-\mu_O^{O\ rich}=\Delta\mu_O(P,T)$. In this paper, we calculate $\Delta\mu_O(P,T)$ using an ideal diatomic gas model with the characteristics of an O_2 molecule,[54] and then relate $\mu_O-\mu_O^{O\ rich}$ to the O_2 pressure P.

III. RESULTS AND DISCUSSION

In this section, we present atomic and electronic structures of the C plane, the R plane, and the A plane of α-Al_2O_3. We restrict ourselves to 1×1 lateral periodicity which is observed experimentally as a stable phase for all planes.

A. C plane: (0001) surface

As shown in Fig. 1(b), there are repeating layer units along the [0001] direction. The layer unit consists of three atomic layers: the Al layer, the O layer, and another Al layer. This unit has no electric dipole moment along the [0001] direction. Figure 2 shows a top view of the Al-I surface of the C plane. In the lateral plane, O atoms form a distorted triangular lattice in which there are two inequivalent equilateral triangles: one is the triangle of which the edges are close to the Al sites A and B, and the other surrounding the Al site C (Fig. 2). Our calculations for bulk α-Al_2O_3 clarify that the side length of the former is 2.89 Å which is longer than that of the latter, 2.54 Å.

1. Energetics

The 1×1 lateral cell has threefold rotational symmetry with the area of 19.90 $Å^2$. BZ integration has been done with 48 $\boldsymbol{k}$ points in the lateral plane of the BZ. The sequence of atomic layers from the top of each surface is shown in Table II.

Figure 3 shows the calculated surface energies as a function of oxygen chemical potential and of oxygen vapor pressure at 1000 K. It is found that the Al-I surface has the lowest surface energy for the possible range of the oxygen chemical potential. Without considering the surface relaxation, the Al-II surface covered by the Al double layer is lowest in energy in the Al-rich environment. Yet the relaxation is important and the energy gains are 123.5 meV/$Å^2$(1.98 J/m^2) for Al-I surface, 20.1 meV/$Å^2$(0.32 J/m^2) for O-I surface, and 2.3 meV/$Å^2$(0.037 J/m^2) for Al-II surface. This difference in the relaxation energy renders the Al-I surface most stable in the whole range of μ_O.

TABLE II. Atomic layer sequence of Al-I, O-I, and Al-II surfaces of the C plane. S and B depict the surface layers and the basic AlO_3Al unit layers, respectively. Each chemical element represents the atomic layer consisting of the corresponding element. Al-I and Al-II surfaces are terminated by single Al layer and double Al layers, respectively, and the outermost layer of O-I surface is the oxygen layer.

	Al-I	O-I	Al-II
S	Al		
	O_3	O_3	
	Al	Al	Al
B	Al	Al	Al
	O_3	O_3	O_3
	Al	Al	Al
	Al	Al	Al
	⋮	⋮	⋮

Table III shows calculated surface energies for the C plane. The surface energies of the Al-II and O-I surfaces depend on the Al and O chemical potentials. For these surfaces, the values in the Al-rich environment for the Al-II and the O-rich environment for the O-I surfaces, respectively, are shown in Table III. For the Al-I surface, surface energies from the previous calculations are available. The previous values are comparable to the value obtained in the present

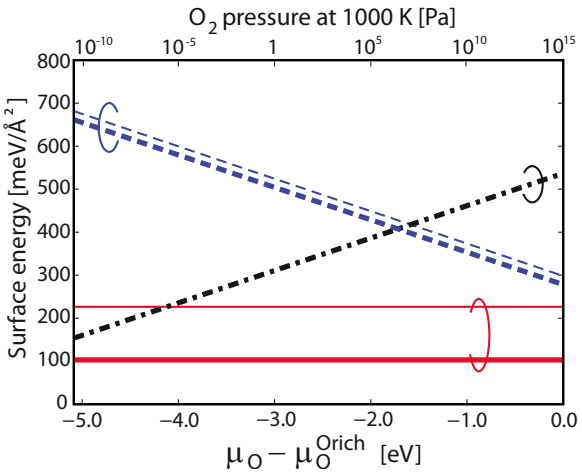

FIG. 3. (Color online) Calculated surface energies for the three surfaces of the C plane. Red solid, blue dashed, and black dashed-dotted lines depict the surface energies of Al-I, O-I, and Al-II surfaces, respectively. Thick (thin) lines show the results for relaxed (unrelaxed) surfaces. The left and right ends of abscissa correspond to the Al-rich and the O-rich environments, respectively.

TABLE III. Surface energies of α-Al_2O_3 in unit of J/m^2. For the nonstoichiometric surfaces the values at either the Al-rich or the O-rich environment are given (see text). In experiments, the observed surface for each plane is not identified, and the experimental values (parenthesized in table) are relative to that of the C (0001).

Plane	Surface	GGA (this work)	GGA[a]	LDA[b]	Expt.[c]
C (0001)	Al-I	1.65	1.98	1.76	(1.00)
	Al-II	2.46			
	O-I	4.46			
R $(1\bar{1}02)$	O-I	1.76	2.04	1.97	(1.05)
	Al-I	2.70			
	O-II	2.70			
	Al-II	2.36			
	O-III	2.12			
A $(11\bar{2}0)$	O-I	2.02	2.34	1.86	(1.12)
	O-II	2.28			
	Al-I	2.67			
	O-III	2.96			
	O-IV	2.79			
	O-V	2.06			

[a]Reference 29.
[b]Reference 20.
[c]Reference 55.

calculation. The accurate surface energies for the three distinctive surfaces obtained in the present work indicate that the C plane experimentally observed is the Al-I surface.

2. Atomic relaxation and electron states of Al-I surface

The Al-I surface is called stoichiometric surface since stoichiometry of Al and O at the top three surface layers is identical to that in bulk Al_2O_3. Calculated atomic coordinates of the Al-I surface are shown in Table IV. One of the prominent features of the surface relaxation is the contraction of the spacing between the top Al and the second O layers. The spacing is found to be reduced by 85% compared with the unrelaxed surface. The fourth Al layer is also relaxed sizably. The contraction of the spacing of atomic layers reduces the atomic distances and hereby gains the energy. In fact, in the unrelaxed geometry, the distances between Al at the top layer and the O at the second are all 1.87 Å, whereas the distances between O at the second and Al at the third and the fourth layers are 1.87 Å and 1.99 Å, respectively. After relaxation, the distance between the topmost Al and the second O becomes 1.70 Å and the distances from the second-layer O to the third and the fourth Al atoms become 1.81 Å and 1.90 Å, respectively.

Atomic relaxation in the lateral plane is minor but not negligible. By analyzing the calculated coordinates in Table IV, it is found that three of the second-layer O atoms move laterally toward the third-layer Al atom to reduce the distances: i.e., the inward breathing relaxation to the third layer Al takes place.

Figure 4 shows calculated energy bands for unrelaxed and relaxed Al-I surface of the C plane. Valence bands of crystalline α-Al_2O_3 are classified in the two groups. The lower valence bands ranging from −19 to −16 eV (relative to the valence-band top) have a character of O 2*s* orbitals, whereas the upper valence bands ranging from −7 to 0 eV have a character of O 2*p* orbitals. Conduction bands of Al_2O_3 mainly consist of Al orbitals. In unrelaxed Al-I surface, we identify seven surface states which are marked in Fig. 4(a). Near the top of the lower valence bands, there are two surface states. Analysis of the corresponding Kohn-Sham orbitals clearly shows that the two states consist of 2*s* orbitals of O atoms located at the second surface layer. In the upper valence-band region, we find four occupied surface states (OSSs) whose amplitudes consist of 2*p* orbitals of O atoms located again at the second surface layer. These surface states are lifted up from corresponding valence bands since less Al atoms which are positively charged are coordinated to the second layer O atoms. Above those states there is an unoccupied surface state (USS) which consists mainly of 3*s* and 3*p* orbitals of the top-layer Al atoms. Since the top-layer Al has less O neighbors than in the bulk, the states which constitute the conduction bands shift downward substantially. Energy gap between the unoccupied and occupied surface states is 0.35 eV for the unrelaxed surface.

TABLE IV. Cartesian coordinates of the unrelaxed structure and the displacements upon relaxation of the Al-I surface of the C plane. All the values are in angstrom. The *x*, *y*, and *z* axes are parallel to $[\bar{2}110]$, $[0\bar{1}10]$, and [0001] directions, respectively.

		Unrelaxed			Relaxed		
Layer	Element	*x*	*y*	*z*	Δx	Δy	Δz
1	Al	4.794	2.768	6.300	0.000	0.000	−0.718
2	O	3.865	1.384	5.456	+0.051	−0.061	+0.009
	O	1.663	0.113	5.456	−0.079	−0.013	+0.009
	O	1.663	2.655	5.456	+0.028	+0.075	+0.009
3	Al	0.000	0.000	4.611	0.000	0.000	−0.021
4	Al	2.397	1.384	4.118	0.000	0.000	+0.200
5	O	3.326	0.000	3.274	−0.023	−0.004	+0.026
	O	0.734	1.271	3.274	+0.008	+0.022	+0.026
	O	3.131	2.881	3.274	+0.015	−0.018	+0.026
6	Al	4.794	2.768	2.429	0.000	0.000	−0.021
7	Al	0.000	0.000	1.936	0.000	0.000	+0.018
8	O	6.262	2.768	1.091	0.000	+0.006	+0.001
	O	4.060	1.497	1.091	+0.005	−0.003	+0.001
	O	4.060	4.039	1.091	−0.006	−0.003	+0.001
9	Al	2.397	1.384	0.247	0.000	0.000	+0.017

Atomic relaxation substantially affects the energy bands [Fig. 4(b)]. Due to the relaxation, the distances from the second-layer O to the neighboring Al atoms are reduced by 3–10 % compared with those in the unrelaxed geometry. Since positively charged Al atoms become close, the surface states consisting of 2*s* and 2*p* orbitals of the second-layer O atoms shift downward merging into the valence bands, although the coordination number of the oxygen is still less compared in the crystal. On the other hand, for the 3*s* and 3*p* orbitals of the top-layer Al, the approach of the negatively

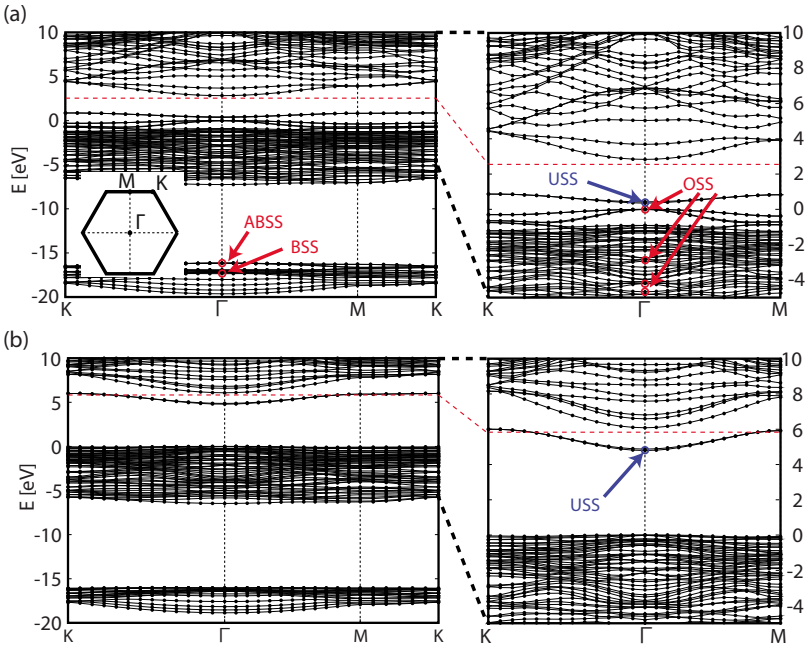

FIG. 4. (Color online) Energy band structures of the Al-I surface of the C plane. Energy bands for (a) the unrelaxed geometry and (b) the relaxed geometry. In (a) and (b), the right panels are extensions of the left panels. A bonding surface state (BSS) and an antibonding surface state (ABSS) are circled in red in left panel. Occupied surface states (OSSs) and an unoccupied surface state (USS) are circled in red and blue, respectively, in right panels. (d) The inset is the surface BZ. States below $E=0$ are occupied. Red dashed horizontal lines denote the vacuum level (see text).

charged O atoms makes the energy levels shift upward. We have indeed found that the unoccupied surface state consisting of Al orbitals shift upward by 3.5 eV [Fig. 4(b)]. The Kohn-Sham orbital of this unoccupied state becomes extended upon the relaxation. We find that the Al-I surface of the C plane has a wide gap of 4.8 eV in GGA, which is consistent with that α-Al_2O_3 surface is experimentally believed to be an insulator.[56] It is noteworthy that this wide gap is realized only after surface atomic relaxation.

In our slab model, the potential between the atomic slabs, i.e., at the middle of the vacuum region, becomes flat. We consider that this flat region corresponds to the vacuum outside α-Al_2O_3. In Figs. 4(a) and 4(b), the vacuum levels thus determined are plotted. The vacuum-level positions are different for the unrelaxed and the relaxed geometries due to the change in the surface dipole potential upon relaxation. We observe several free-electronlike states which are distributed in the vacuum region above the vacuum level. By comparing the energy bands of crystalline α-Al_2O_3 and of the Al-I surface, we can identify the bulk conduction-band states in Figs. 4(a) and 4(b). It is revealed that bulk conduction-band states are located above the vacuum level, indicating that the C plane of α-Al_2O_3 has negative electron affinity.

3. Nonstoichiometric Al-II and O-I surfaces

The Al-II and O-I surfaces are called nonstoichiometric surfaces. Our calculations show that the surface energies of the Al-II and the O-I are higher by 51 meV/Å^2(0.81 J/m^2) in the Al-rich condition and by 175 meV/Å^2(2.81 J/m^2) in the O-rich condition, respectively, than the Al-I surface energy. The Al-II surface is of interest since peculiar Al-rich structures emerge at high temperature[10] or in ultrathin films.[32,33]

We have performed structural optimization of the Al-II surface, and found that, in contrast to the Al-I surface, the atomic relaxation is unimportant: The maximum displacements of the surface atoms from the unrelaxed geometries is found to be less than 0.08 Å after our extensive geometry optimization. This results in the small relaxation energy of the Al-II surface (2.3 meV/Å^2) as shown in the previous section. Consequently, the energy bands of the unrelaxed and the relaxed A-II surfaces are similar to each other. We have found two surface states in the energy gap: One is completely and the other is partly occupied. The Al-II surface is therefore metallic. Both surface states consist of $3s$ and $3p$ orbitals of Al atoms located at the two topmost layers (Fig. 5). The lower and the upper surface states are the bonding and the antibonding states, respectively.

In the O-II surface, significant displacements of Al atoms are absent. Instead, large displacements (0.49 Å) of the top-

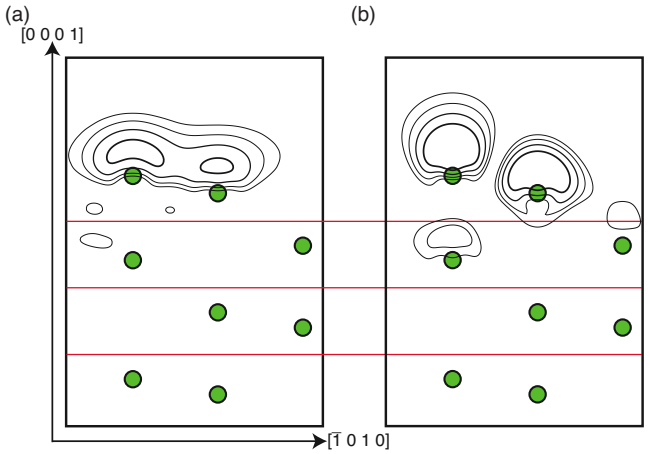

FIG. 5. (Color online) Contour plots of squared Kohn-Sham orbitals of (a) the lower and (b) the upper surface states at Γ point of the relaxed Al-II surface of the C plane. Green circles represent the Al atoms and red horizontal lines indicate the O layers. The innermost contour lines correspond to the value 0.02 electron/Å^3 and each contour represents twice or half the value of the adjacent line.

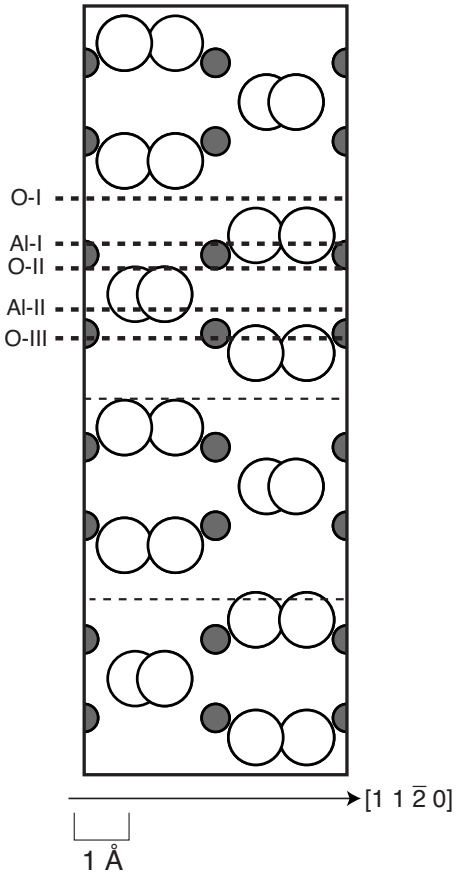

FIG. 6. Atomic arrangements of α-Al_2O_3 along the $[\bar{1}101]$ direction. The vertical axis is perpendicular to the R plane. Large white and small gray circles depict oxygen and aluminum atoms, respectively. Horizontal thick dashed lines represent five distinctive surfaces, the O-I, the Al-I, O-II, Al-II, and O-III surfaces, of the R plane.

layer O atoms mainly in the lateral plane are found. These displacements make the triangular lattice of the topmost oxygen layer distorted. The sides of the smaller triangles decrease from 2.54 to 2.25 Å and the triangles rotate by 18° clockwise.

We have calculated energy bands (not shown here) and found four surface states consisting of the top-layer O atoms. The states near the top of the lower valence bands have a character of O 2*s* orbitals, whereas the states near the top of the upper valence bands have a character of O 2*p* orbitals. The surface states remain in the energy gap after the atomic relaxation: The relaxation is insufficient to erase the surface states from the energy gap. We have found that there is a wide gap of 6.3 eV between the O 2*p* surface state and the conduction band bottom.

The Al-II and the O-I surfaces are nonstoichiometric. As a consequence, there is excess or lack of electrons to make all the atoms closed shell as in the perfect crystal. Hence there exist partially occupied surface states around the Fermi level. When there is an electron reservoir, e.g., a metal contact on the surface, or when the specimen is under, e.g., LEED experiments, or when some acceptors or donors are introduced, electrons are supplied to or removed from the surface and the surface may be charged. This charged surface is a polar surface in Tasker's sense.[57] In the polar surface, the net dipole moment and thus the electrostatic potential increase monotonically with increasing thickness of the films, and thereby the surface energy diverges. Hence it is unlikely that the Al-II and the O-I surface appears when the electron reservoir exists.

TABLE V. Atomic layer sequence of O-I, Al-I, O-II, Al-II, and O-III surfaces of the R plane. S and B represent the surface layer and the basic $O_2Al_2O_2Al_2O_2$ unit layer, respectively.

	O-I	Al-I	O-II	Al-II	O-III
S	O_2				
	Al_2	Al_2			
	O_2	O_2	O_2		
	Al_2	Al_2	Al_2	Al_2	
	O_2	O_2	O_2	O_2	O_2
B	O_2	O_2	O_2	O_2	O_2
	Al_2	Al_2	Al_2	Al_2	Al_2
	O_2	O_2	O_2	O_2	O_2
	Al_2	Al_2	Al_2	Al_2	Al_2
	O_2	O_2	O_2	O_2	O_2
	O_2	O_2	O_2	O_2	O_2
	⋮	⋮	⋮	⋮	⋮

B. R plane: $(1\bar{1}02)$ surface

Figure 6 shows atomic arrangements of α-Al_2O_3 along the $[\bar{1}101]$ direction, representing a side view of the $(1\bar{1}02)$ surface, i.e., the R plane. The 1×1 lateral unit of the R plane is constructed of two primitive vectors along the directions of $[11\bar{2}0]$ and $[\bar{1}101]$. There is a layer unit consisting of five atomic layers (Fig. 6): an O layer constructed of two O atoms in the 1×1 unit, an Al layer constructed of two Al atoms, an O layer constructed of two O atoms, an Al layer constructed of two Al atoms, and an O layer constructed of two O atoms. This O_2-Al_2-O_2-Al_2-O_2 repeating-layer unit has no dipole moment along the direction perpendicular to the R plane. There are five distinctive ways of termination of α-Al_2O_3 in the R plane, leading to five different surfaces shown in Fig. 6: they are called O-I, Al-I, O-II, Al-II, and O-III surfaces of the R plane hereafter.

1. Energetics

The area of the 1×1 lateral cell is 24.78 $Å^2$. BZ integration has been done with 4×4 $\boldsymbol{k}$ points in the lateral plane of the BZ. We have calculated stable atomic structures, corresponding surface energies and electron states of the O-I, Al-I, O-II, Al-II, and O-III surfaces. The sequence of atomic layers from the top of each surface is shown in Table V. Figure 7 shows the calculated surface energies as a function of oxygen chemical potential and of oxygen vapor pressure. It is found that the O-I surface has the lowest surface energy for the possible range of the oxygen chemical potential. We have

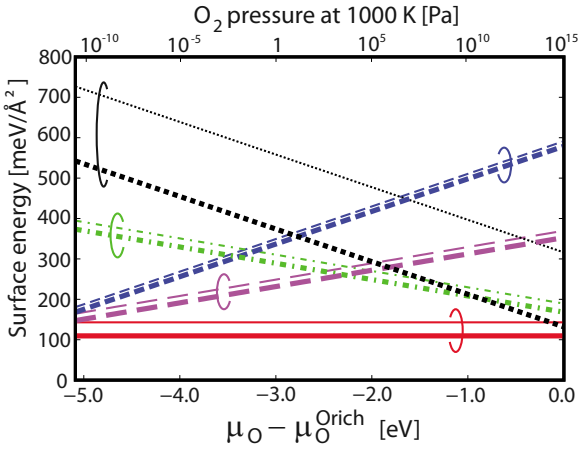

FIG. 7. (Color online) Calculated surface energies for the five surfaces of the R plane. Red solid, blue dashed, green dashed-dotted, purple long-dashed, and black dotted lines depict the surface energies of O-I, Al-I, O-II, Al-II, and O-III surfaces, respectively. Thick (thin) lines show the results for relaxed (unrelaxed) surfaces. The left and right ends of abscissa correspond to the Al-rich and the O-rich environments, respectively.

also investigated other structures made by adding or removing atoms but the surface energies of those surfaces are higher than the surface energy of the O-I surface. It is thus likely that the R plane experimentally observed is this O-I surface.

The energy gain upon relaxation for the O-I surface is 34 meV/Å^2, whereas the gain for the O-III surface is much larger, 184 meV/Å^2. Hence the surface energy of the O-III becomes close to that of the O-I after relaxation in the O-rich environment. The surface energy of the Al-II surface is comparable to that of the O-I surface in the Al-rich environment. On Al-II surface, bonds consisting of $3p$ orbitals of surface Al atoms are formed, and this bond formation keeps the surface Al atoms close to the unrelaxed positions. This reflects on relatively small relaxation energy 17 meV/Å^2 on the Al-II surface. This feature is similar to the Al-II surface of the C plane.

In Table III, the calculated surface energies of the relaxed five surfaces of the R plane are listed. The surface energies of the Al-I, O-II, Al-II, and O-III depend on the Al and O chemical potentials. For these surfaces, the values in the Al-rich environment for the Al-I and Al-II surfaces, and the values in the O-rich environment for the O-II and O-III surfaces, respectively, are shown in Table III. The calculated ratio of the surface energy of the most stable surface of the R plane to that of the C plane is 1.07 in the present calculation, which is in agreement with the experimental value, 1.05. In the followings, we concentrate on the two surfaces: the most stable O-I surface and the metastable O-III surface which shows the large relaxation energy.

2. Atomic relaxation and electron states of O-I surface

The calculated atomic positions of the O-I surface are shown in Table VI. The atomic relaxation is not as significant as in the Al-I surface of the C plane. Yet it is certainly sizable. The distances between the O atom on the topmost layer and two Al atoms in the second layer and one Al atom in the fourth layer become 1.78 Å (4.6% reduction), 1.84 Å (7.3% reduction), and 1.95 Å (1.7% reduction), respectively, after the relaxation.

TABLE VI. Cartesian coordinates of the unrelaxed structure and the displacement in the atomic relaxation of the O-I surface of the R plane. All the values are in angstrom. The x and y axes are parallel to $[11\bar{2}0]$ and $[\bar{1}101]$ directions, respectively. The z axis is perpendicular to the R plane.

		Unrelaxed			Relaxed		
Layer	Kind	x	y	z	Δx	Δy	Δz
1	O	0.734	3.783	6.333	+0.040	+0.082	−0.040
	O	1.663	6.367	6.333	−0.040	+0.082	−0.040
2	Al	0.000	5.594	5.976	+0.141	−0.048	−0.091
	Al	2.397	3.009	5.976	−0.141	−0.048	−0.091
3	O	3.326	4.464	5.259	+0.011	−0.015	+0.115
	O	3.865	1.880	5.259	−0.011	−0.015	+0.115
4	Al	4.794	3.334	4.543	−0.019	−0.018	+0.052
	Al	2.397	5.918	4.543	+0.019	−0.018	+0.052
5	O	0.734	5.145	4.186	+0.008	+0.021	−0.046
	O	1.663	2.560	4.186	−0.008	+0.021	−0.046
6	O	3.131	6.007	2.827	+0.007	−0.007	+0.032
	O	4.060	3.422	2.827	−0.007	−0.007	+0.032
7	Al	2.397	2.649	2.470	+0.001	−0.004	−0.006
	Al	0.000	5.233	2.470	−0.001	−0.004	−0.006
8	O	1.468	4.103	1.753	−0.004	−0.006	−0.017
	O	0.929	6.687	1.753	+0.004	−0.006	−0.017
9	Al	4.794	2.973	1.037	+0.005	−0.003	+0.001
	Al	2.397	5.558	1.037	−0.005	−0.003	+0.001
10	O	4.060	4.784	0.680	−0.005	−0.007	+0.009
	O	3.131	2.200	0.680	+0.005	−0.007	+0.009

The calculated energy bands for the O-I surface are shown in Fig. 8. Several surface states appear above the lower and the upper valence bands, i.e., at around −15 and 0 eV. These surface states are occupied and their Kohn-Sham orbitals are found to have large amplitudes at the topmost O layer (Fig. 9). It is found that the two surface states around −15 eV are

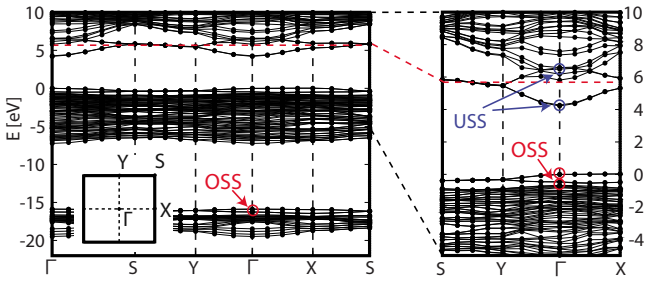

FIG. 8. (Color online) Energy band structures of the O-I surface of the relaxed R plane. The right panels are extensions of the left panels. The inset shows the surface BZ. OSS and USSs are circled in red and blue, respectively. States below E=0 are occupied. Red dashed horizontal lines denote the vacuum level.

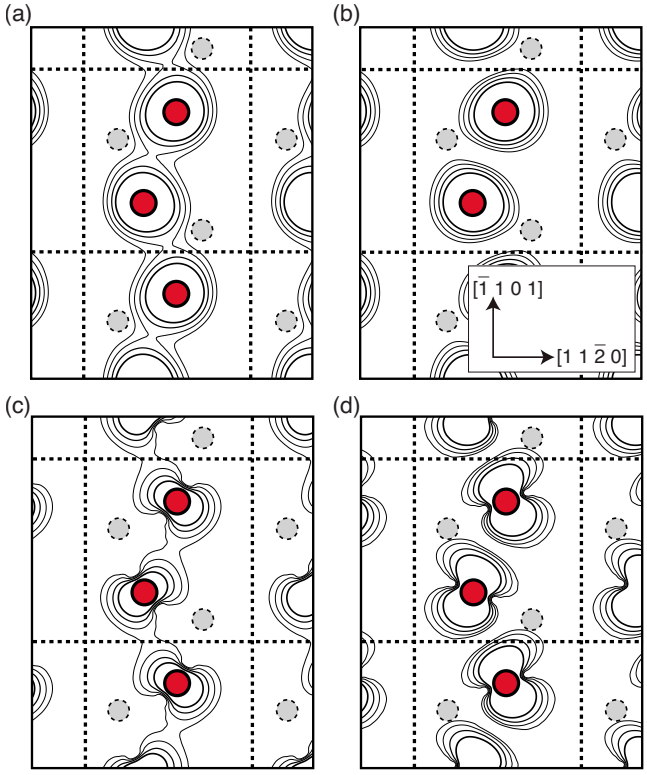

FIG. 9. (Color online) Contour plots of the squared Kohn-Sham orbitals of the occupied surface states on the O-I surface of the R plane. (a) The bonding and (b) the antibonding states located below −15 eV and circled in red in the left panel of Fig. 8, and the states [(c) and (d)] located at around 0 eV and circled in red in the right panel of Fig. 8. The plane is parallel to the surface and contains the topmost oxygen layer. Circles and dashed lines depict the O atoms and the lateral unit cell, respectively. Gray broken-line circles depict Al atoms in the second layer which are located 0.36 Å below the topmost O layer. The innermost contour lines correspond to the value 0.02 electron/Å^3 and each contour represents twice or half the value of the adjacent line.

the bonding and the antibonding characters consisting of 2*s* orbitals of the top-layer O atoms, whereas other two surface states around 0 eV consist of 2*p* orbitals of the O atoms. The coordination number of the O atoms on the topmost layer is reduced. This makes the energy levels of the O orbitals at the top-layer shift upward, and thus the above four surface states appear near the top of the corresponding valence bands. The atomic relaxation reduces the distances between the threefold coordinated O atoms and neighboring Al atoms by 2–7 %. This reduction in the distance to the positively charged Al atoms makes the energy levels of the O orbitals lower and thus the energy levels of these occupied surface states shift downward. Yet in contrast with the case of the Al-I surface of the C plane, the surface states remain above the valence bands even after the relaxation. This difference is explained as follows: In the case of the Al-I surface of the C plane, the Al atom on the topmost layer can freely move to decrease the Al-O distances because of the absence of the upper layers. On the R plane, on the other hand, the displacement of Al atoms in the second layer is suppressed by the Al-O ionic bonds with the lower layer and thus insufficient to make the surface states merge into the valence bands.

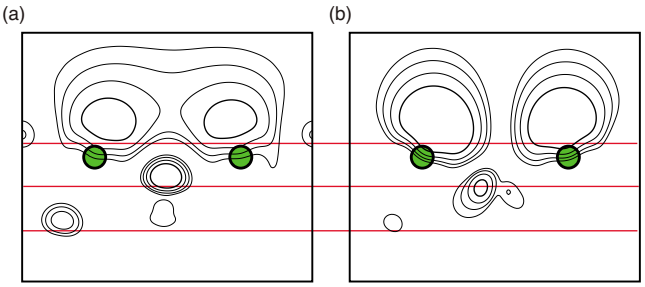

FIG. 10. (Color online) Contour plots of the squared Kohn-Sham orbitals of the USSs on the O-I surface of the R plane. The two orbitals, (a) and (b), correspond to the two USSs circled in blue in the right panel of Fig. 8 in order of increasing energy. Green circles and red horizontal lines depict the Al atoms and the O layers, respectively. The horizontal axis is along the line connecting two Al atoms in the second layer and the vertical axis is perpendicular to the R plane. The innermost contour lines correspond to the value 0.02 electron/Å^3 and each contour represents twice or half the value of the adjacent line.

We have also found unoccupied surface states in the original band gap of α-Al_2O_3. They consist mainly of Al orbitals located in the second-layer (Fig. 10). It is clear that these unoccupied surface states consist mainly of 3*s* and 3*p* orbitals of the second-layer Al atoms. The lower and the upper states correspond to the bonding and the antibonding states, respectively. This formation of the bonds near the surface is similar to the case of the Al-II surface of the C plane, thus revealing the covalent nature on the surface of the ionic materials. The energy levels of these surface states shift upward upon the atomic relaxation. This feature is the same as the case of the Al-I surface of the C plane: The decrease in the Al-O distances causes an increase in the on-site energy of the Al atom due to the negatively charged O atoms, and therefore the surface states made from Al orbitals shift upward.

The vacuum levels represented by broken horizontal lines in Fig. 8 are determined by the potential energy in the vacuum region in our slab model. The conduction-band states of crystalline Al_2O_3 are located above the vacuum level. This indicates that the R plane has negative electron affinity, as the C plane does.

3. Molecule formation on O-III surface

We next present atomic structures and electron states of the O-III surface on which an oxygen molecular unit is spontaneously formed. The O atoms on the top and the second layers are singly and threefold coordinated, respectively, to Al atoms in the unrelaxed geometry. On the other hand, all the Al atoms are sixfold coordinated as they are in the perfect crystal. The top views of the unrelaxed and the relaxed O-III surface is shown in Fig. 11. From this figure, we clearly recognize that the oxygen atoms in the topmost layer move significantly in the lateral plane. As a result, the distance between the two O atoms on the top layer is reduced to 1.27 Å from 2.75 Å. This short distance is close to the bond length of an oxygen molecule, 1.21 Å.

The calculated energy band structures are shown in Fig. 12. The overall feature of the energy bands of the unrelaxed

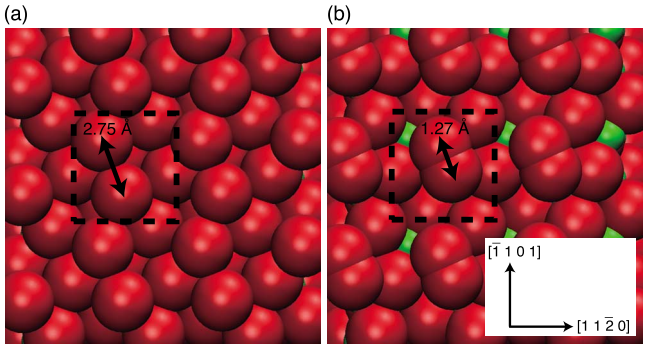

FIG. 11. (Color online) Top view of (a) the unrelaxed and (b) the relaxed structures of the O-III surface of the R plane. Large red and small green spheres denote the O and the Al atoms, respectively. The broken-line square indicates 1×1 lateral unit of the R plane.

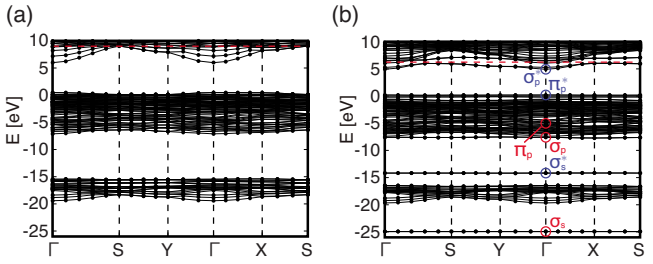

FIG. 12. (Color online) Energy band structures of the O-III surface of the R plane; those (a) of the unrelaxed structure and (b) of the relaxed structure. States below $E=0$ are occupied. Red dashed horizontal lines indicate vacuum levels. Circles in (b) represent the bonding and the antibonding states of the O-O unit on the topmost layer.

O-III surface is similar to the energy bands of the perfect crystal. Upon relaxation, however, several localized states appear. They are marked in Fig. 12(b).

The contour plots of these localized states are shown in Fig. 13. It is clearly shown that an O-O covalent bond is formed on the surface. The character of this bond is the same as the bond of an oxygen molecule: i.e., the Kohn-Sham orbitals of these localized states have the character of σ_s, σ_s^*, σ_p, π_p, π_p^*, and σ_p^* states, as they are in an isolated oxygen molecule.

The desorption energy of this O-O unit is 0.5 eV in our spin-unpolarized calculations, i.e., this O-O unit stays on the O-III surface. In spin-polarized calculations, however, the energy of the O-III surface is higher than the configuration in which the O_2 is desorbed. Hence, when the spin is flipped on the surface, the O-O unit desorbs from the surface as an oxygen molecule, and the surface structure becomes the O-I surface discussed previously. This may be a reason for the fact that oxygen adsorption on the Al_2O_3 surface is difficult.

C. A plane: $(11\bar{2}0)$ surface

Figure 14(a) shows atomic arrangements of α-Al_2O_3 along the direction perpendicular to the plane constructed of two vectors along $[2\bar{2}01]$ and the $[11\bar{2}0]$, representing a side view of the $(11\bar{2}0)$ surface, i.e., the A plane. The 1×1 lateral unit of the A plane is constructed of two primitive vectors along the directions of $[\bar{1}101]$ and $[2\bar{2}01]$. Along the $[11\bar{2}0]$ direction, there is a layer unit consisting of five atomic layers: an O layer constructed of one O atom in the 1×1 unit, an O layer constructed of two O atoms, an Al layer constructed of four Al atoms, an O layer constructed of two O atoms, and an O layer constructed of one O atoms. This O-O_2-Al_4-O_2-O repeating layer unit has no dipole moment along the $[11\bar{2}0]$ direction. There are five distinctive ways of termination of α-Al_2O_3 in the A plane, leading to five different surfaces shown in Fig. 14(a): They are called the O-I, O-II, Al-I, O-III, and O-IV surfaces of the A plane hereafter. In addition to the five surfaces above, we have also investigated another surface structure. This additional structure named O-V surface is shown in Fig. 14(b). The O-V surface is constructed by removing one oxygen atom [labeled by star in Fig. 14(a)] from the topmost layer of the O-III surface.

1. Energetics

The area of the 1×1 lateral cell is 36.24 Å^2. BZ integration has been done with 4×2 $\boldsymbol{k}$ points in the lateral plane of the BZ. We have calculated stable atomic structures, corresponding surface energies and electron states of O-I, O-II, Al-I, O-III, O-IV, and the O-V surfaces. The sequence of atomic layers from the top of each surface is shown in Table VII.

Figure 15 shows the calculated surface energies as a function of oxygen chemical potential and of the O_2 pressure. It

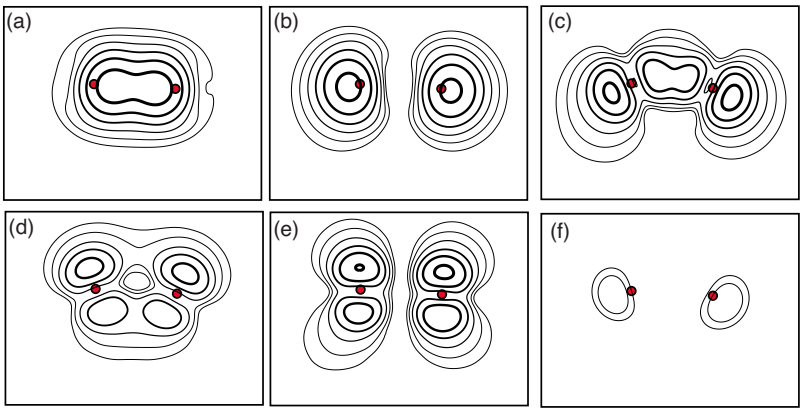

FIG. 13. (Color online) Contour plots of the squared Kohn-Sham orbitals of the surface states on the relaxed O-III surface of the R plane. The six orbitals from (a) to (f) corresponds to the states circled in Fig. 12 in the order of increasing energy. Red circles indicate the O atoms, which form the covalent bond, on the O-III surface. The outermost contour lines correspond to the value 0.0125 electron/Å^3 and each contour represents twice or half the value of the adjacent line. Horizontal direction is along the O-O covalent bond and vertical direction is perpendicular to the surface.

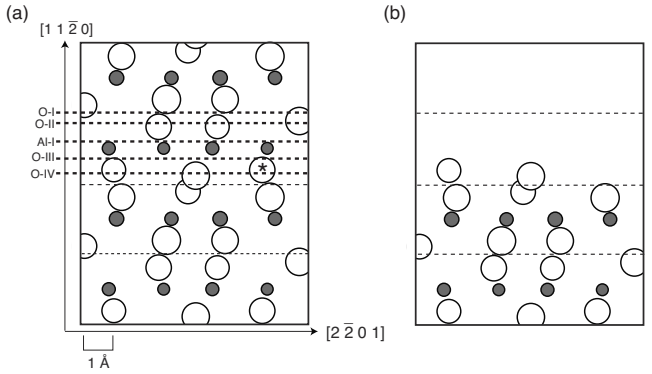

FIG. 14. (a) Atomic arrangements of α-Al_2O_3 along the direction perpendicular to the plane constructed of two vectors along $[2\bar{2}01]$ and the $[11\bar{2}0]$. Large white and small gray circles depict oxygen and aluminum atoms, respectively. Horizontal lines represent five distinctive surfaces, O-I, O-II, Al-I, O-III, and O-IV surfaces, of the A plane. (b) Side view of the O-V surface of the A plane.

is found that the O-I surface has the lowest surface energy for the possible range of the oxygen chemical potential. It is thus likely that the A plane experimentally observed is this O-I surface.

In relaxed structures, the surface energy of the O-V surface is very close to the value of the most stable O-I surface in the O-rich environment. This is the consequence from large relaxation energy of the O-V surface, which is calculated to be 133 meV/Å^2 and much larger than the corresponding value, 45 meV/Å^2 for the O-I surface. The surface energy of Al-I surface is almost the same with that of the O-I surface in the unrelaxed geometries in the Al-rich environment. Yet the relaxation energy of the Al-I surface of the A plane is 30 meV/Å^2 which is smaller than that of the O-I surface. This situation is similar to the case of the Al-II surface of the C plane, where bonds between the surface Al atoms are formed and thus prevent the surface Al atoms from sinking toward subsurface layers.

TABLE VII. Atomic layer sequence of O-I, O-II, Al-I, O-III, O-IV, and O-IV surfaces of the A plane. S and B depict the surface layer and the basic $OO_2Al_4O_2O$ unit layer, respectively.

	O-I	O-II	Al-I	O-III	O-IV	O-V
S	O					
	O_2	O_2				
	Al_4	Al_4	Al_4			
	O_2	O_2	O_2	O_2		O
	O	O	O	O	O	O
B	O	O	O	O	O	O
	O_2	O_2	O_2	O_2	O_2	O_2
	Al_4	Al_4	Al_4	Al_4	Al_4	Al_4
	O_2	O_2	O_2	O_2	O_2	O_2
	O	O	O	O	O	O
	O	O	O	O	O	O
	⋮	⋮	⋮	⋮	⋮	⋮

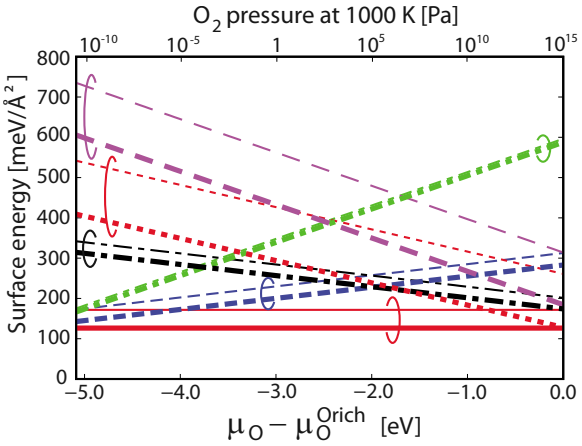

FIG. 15. (Color online) Calculated surface energies for the six surfaces of the A plane. Red solid, blue dashed, green dashed-dotted, purple long-dashed, black long-dashed-dotted, and red dotted lines depict the surface energies of O-I, O-II, Al-I, O-III, O-IV, and O-V surfaces, respectively. Thick (thin) lines show the results for relaxed (unrelaxed) surfaces. The left and right ends of abscissa correspond to the Al-rich and the O-rich environments, respectively.

In Table III, the calculated surface energies of the relaxed six surfaces of the A plane are listed. We list the surface energies in the Al-rich environment for the O-II and Al-I surfaces, and energies in the O-rich environment for the O-III, the O-IV, and the O-V surfaces, respectively, in Table III. The calculated ratio of the surface energy of the most stable surface of the A plane to that of the C plane is 1.22 in the present calculation, which is in fair agreement with the experimental value, 1.12. In the following sections, We will discuss the two surfaces: the most stable O-I surface and the O-V surface which has the large relaxation energy.

2. Atomic relaxation and electron states of O-I surface

The calculated atomic positions of O-I surface of the A plane is shown in Table VIII. The atomic displacements upon relaxation are not prominent. Yet the relaxation reduces the distances between the surface O atom and neighboring Al atoms sizably: the distances between the O atom in the top layer and two Al atoms in the third layer become 1.73 Å which is the 7.3% reduction. The distances between the O atom in the second layer and three Al atoms in the third layer become 1.81 Å (3.4% reduction), 1.92 Å (3.3% reduction), and 1.85 Å (7.0% reduction), respectively, upon relaxation.

The calculated energy band structures are shown in Fig. 16. We have found several surface states appear near tops of the lower and the upper valence bands (at around −15 and 0 eV). There are also unoccupied surface states in the original band gap. Figure 17 shows the contour plots of the occupied and the unoccupied surface states on the O-I surface of the A plane. It is found that the occupied surface states below −15 eV have the character of the 2*s* orbitals of the top and the second O layers. The unoccupied surface states, on the other hand, have the character of 3*s* and 3*p* orbitals of the third-layer Al atoms. The coordination number of the O atoms on the top and the second layers are reduced from the bulk value 4 to 2 and 3, respectively. The relaxation changes

TABLE VIII. Cartesian coordinates of the unrelaxed structure and the displacements in atomic relaxation of the O-I surface of the A plane. All the values are in angstrom. The x and z axes are parallel to $[\bar{1}101]$ and $[11\bar{2}0]$ directions. The y axis is perpendicular to x and z axes.

		Unrelaxed			Relaxed		
Layer	Kind	x	y	z	Δx	Δy	Δz
1	O	1.653	3.506	7.101	0.000	0.000	−0.002
2	O	3.196	1.073	6.905	+0.055	−0.013	−0.054
	O	5.278	5.939	6.905	−0.055	+0.013	−0.054
3	Al	5.006	0.717	6.171	−0.106	−0.048	−0.055
	Al	3.107	2.790	6.171	−0.194	−0.076	+0.040
	Al	5.367	4.223	6.171	+0.194	+0.076	+0.040
	Al	3.468	6.296	6.171	+0.106	+0.048	−0.055
4	O	4.918	2.433	5.438	−0.004	+0.021	+0.106
	O	3.556	4.580	5.438	+0.004	−0.021	+0.106
5	O	1.292	0.000	5.242	0.000	0.000	+0.093
6	O	4.598	7.013	4.704	0.000	0.000	−0.096
7	O	0.972	4.580	4.508	+0.019	+0.009	−0.026
	O	2.334	2.433	4.508	−0.019	−0.009	−0.026
8	Al	2.783	4.223	3.774	+0.017	−0.007	+0.053
	Al	0.523	2.790	3.774	−0.017	+0.007	+0.053
	Al	0.884	6.296	3.774	+0.006	−0.016	−0.034
	Al	2.422	0.717	3.774	−0.006	+0.016	−0.034
9	O	2.694	5.939	3.040	+0.005	+0.005	+0.021
	O	0.611	1.073	3.040	−0.005	−0.005	+0.021
10	O	4.237	3.506	2.845	0.000	0.000	+0.029
11	O	1.653	3.506	2.307	0.000	0.000	0.000
12	O	5.278	5.939	2.111	+0.002	−0.003	−0.022
	O	3.196	1.073	2.111	−0.002	+0.003	−0.022
13	Al	5.006	0.717	1.377	−0.002	+0.009	−0.003
	Al	3.468	6.296	1.377	+0.002	−0.009	−0.003
	Al	3.107	2.790	1.377	−0.010	+0.014	+0.006
	Al	5.367	4.223	1.377	+0.010	−0.014	+0.006
14	O	4.918	2.433	0.643	−0.001	+0.007	+0.007
	O	3.556	4.580	0.643	+0.001	−0.007	+0.007
15	O	1.292	0.000	0.448	0.000	0.000	+0.013

distances between such twofold coordinated O atoms and neighboring Al atoms, from 1.87 Å and 1.87 Å to 1.73 Å and 1.73 Å, respectively, and also changes distances between threefold coordinated O atoms and neighboring Al atoms from 1.87 Å, 1.99 Å, and 1.99 Å to 1.81 Å, 1.92 Å, and 1.85 Å, respectively. Although the coordination numbers of these O atoms are still less than four, this reduction in the distances to the positively charged Al atoms makes the energy level of the O orbitals lower. Yet, in contrast with the case of the Al-I surface of the C plane, several states remain above the valence bands. The situation is similar to the O-I surface of the R plane.

The unoccupied surface states mainly consist of the atomic orbitals of the Al atoms in the third layer [Figs. 17(c) and 17(d)] and the energy level of these states shift upward upon atomic relaxation. This feature is the same as the case of the Al-I surface of the C plane: i.e., the decrease in Al-O distances, which is a consequence of the ionic total-energy

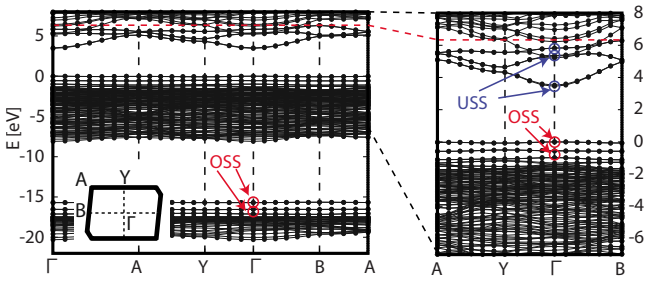

FIG. 16. (Color online) Energy band structures of the O-I surface of the A plane. The right panels are extensions of the left panels. The inset shows the surface BZ. OSS and USS are circled in red and blue, respectively. States below E=0 are occupied. Red dashed horizontal lines denote the vacuum level.

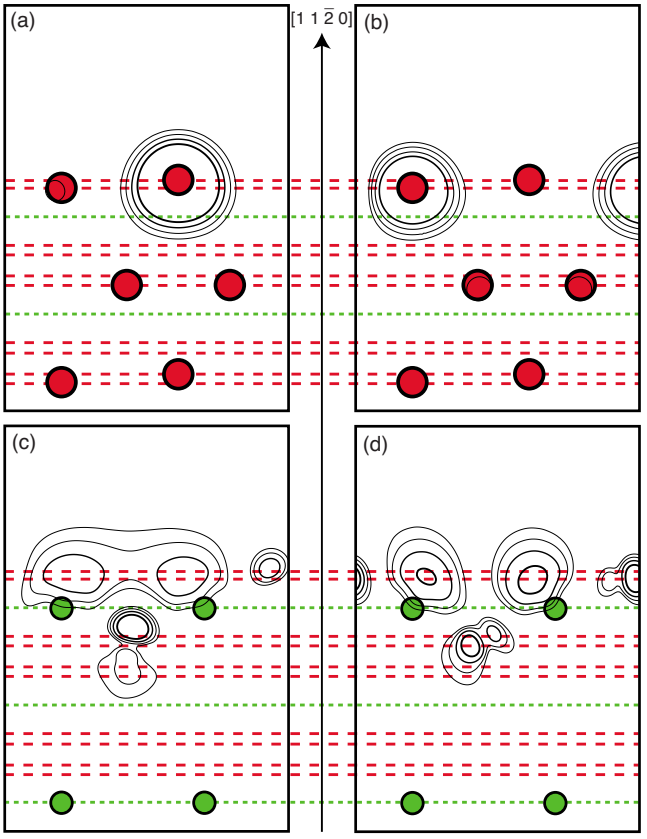

FIG. 17. (Color online) Contour plots of the squared Kohn-Sham orbitals of the occupied and the unoccupied surface states on the O-I surface of the A plane. (a) and (b): the OSSs circled in red in the left panel of Fig. 16; the plane includes the O atoms in the top and second layers. (c) and (d): the USSs circled in blue in the right panel of Fig. 16; the plane includes two Al atoms in the third layer. Red circles in (a) and (b) depict the O atoms, whereas green circles depict Al atoms in (c) and (d). Red broken and green dotted lines indicate the positions of the oxygen and the aluminum atomic layers, respectively. The innermost contour lines correspond to the value 0.02 electron/Å^3 and each contour represents twice or half the value of the adjacent line.

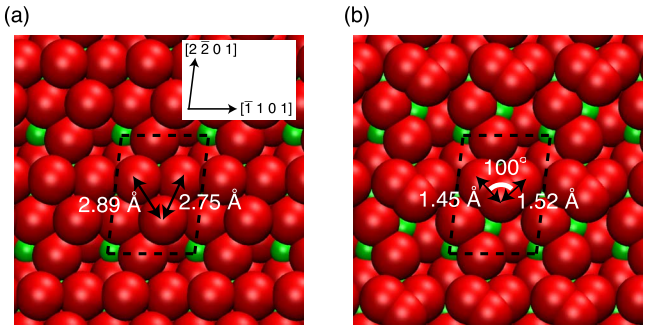

FIG. 18. (Color online) Top view of (a) the unrelaxed and (b) the relaxed structures of the O-V surface of the A plane. Large red and small green spheres indicate the O and the Al atoms, respectively. Broken-lined parallelograms indicate 1×1 lateral unit of the A plane.

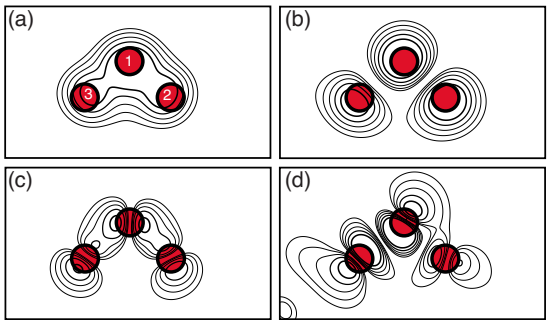

FIG. 19. (Color online) Contour plots of the squared Kohn-Sham orbitals of the four surface states on the relaxed O-V surface of the A plane. The four states are located in energy at −23.1, −14.3, −7.3, and 2.7 eV relative to the valence-band top. Red circles indicate the O atoms, which form the covalent bond, on the O-V surface. The numbers 1, 2, and 3 in (a) indicate the O atom in the first, second, and the third layers of the O-V surface, respectively. The plane shown includes these three oxygen atoms. The innermost contour lines correspond to the value 0.1 electron/Å^3 and each contour represents twice or half the value of the adjacent line.

gain, causes an increase in the on-site energy of the Al atom and therefore the surface states made from the Al orbitals shift upward.

3. Formation of ozone on the O-IV surface

We finally present atomic structures and electron states of the O-V surface of the A plane. The O atoms on the top, the second, and the third layers are singly, doubly, and triply coordinated, respectively, to Al atoms. The top views of the unrelaxed and the relaxed O-V surface is shown in Fig. 18. From this figure, we clearly recognize that the O atoms in the topmost layer move significantly in the lateral plane. As a result, the three oxygen atoms gather and form O-O covalent bonds. The shape of this O_3 unit is similar to an ozone molecule. The two O-O bond distances are 1.45 and 1.52 Å and the bond angle is 100° which are comparable with the corresponding values of an isolated ozone molecule, 1.27 Å and 117°.[58]

The overall features of the calculated energy bands of the unrelaxed O-IV surface and those of the perfect crystal are similar to each other (not shown). In the relaxed structure, however, there appear clear surface states. The contour plots of these surface states are shown in Fig. 19. It is found that O-O covalent bonds are formed on the surface. The characters of these bonds are similar to the bonds of ozone molecule.

Peeling this O_3 unit from the surface requires a large energy cost of 7 eV, indicating that it is unlikely that the ozone unit desorbs from the O-V surface. To examine the stability of the O_3 unit, we next consider a possibility of the desorption of an O_2 unit consisting of the top and the second layer O atoms. In spin-polarized calculations, we have found that the O_2 unit which constitutes the O_3 unit desorbs from the surface without energy barrier. Hence, when there is a spin-inversion process available, the O_3 unit desorbs from the O-V surface, resulting in the appearance of the O-I surface on the A plane.

IV. SUMMARY

We have performed total-energy electronic-structure calculations for three important surfaces, C plane [the (0001) surface], R plane [the $(1\bar{1}02)$ surface], and A plane [the $(11\bar{2}0)$ surface], of α-Al_2O_3 on the basis of the generalized gradient approximation in the density-functional theory. Each plane has several distinctive surface terminations with different stoichiometry for which we have carried out detailed calculations to reveal surface atomic relaxations, surface energies, and electronic structures. We have found that the stoichiometric surface of the C plane has the lowest surface energy, followed by the stoichiometric surfaces of the R plane and then the A plane, irrespective of the chemical potentials of constituting elements. Detailed atomic structures for stable and metastable surfaces of each plane has been obtained, which is imperative for atom-scale clarification of reactions on the α-Al_2O_3 surface. The electron states of each surface have been calculated in detail. The obtained surface energy bands offer a possibility to identify atomic structures of α-Al_2O_3 surface by spectroscopic measurements. Accurate determination of the atomic arrangements presented in this paper, along with the corresponding surface electron states, has unraveled each role of ionicity, metallicity, and then covalency in surfaces of α-Al_2O_3, a representative of metal oxides. This contributes to atom-scale quantitative identification and characterization of the important surfaces of Al_2O_3, which are lacking in the past from science viewpoints in contrast with its technological importance. This also provides a firm theoretical framework to consider atomically controlled growth or deposition of important active materials on Al_2O_3 which has been used so far just because of its hardness against harsh environments.

ACKNOWLEDGMENTS

Computations were done at Academic Computing & Communications Center, University of Tsukuba, at Institute for Solid State Physics, University of Tokyo, and at Research Center for Computational Science, Okazaki, Japan.

*Present address: Research and Development Center, Toshiba Corporation.
†Corresponding author; oshiyama@ap.t.u-tokyo.ac.jp

[1] H. Amano, N. Sawaki, I. Akasaki, and Y. Toyoda, Appl. Phys. Lett. **48**, 353 (1986).
[2] R. Di Felice and J. E. Northrup, Appl. Phys. Lett. **73**, 936 (1998).
[3] H. Ago, K. Nakamura, K. Ikeda, N. Uehara, N. Ishigami, and M. Tsuji, Chem. Phys. Lett. **408**, 433 (2005).
[4] S. Han, X. Kiu, and C. Zhou, J. Am. Chem. Soc. **127**, 5294 (2005).
[5] N. Ishigami, H. Ago, K. Imamoto, M. Tsuji, K. Iakoubovski, and N. Minami, J. Am. Chem. Soc. **130**, 9918 (2008).
[6] V. E. Heinrich and P. A. Cox, *Surfaces of Metal Oxides* (Cambridge University Press, Cambridge, 1994).
[7] T. M. French and G. A. Somorjai, J. Phys. Chem. **74**, 2489 (1970).
[8] G. Renaud, B. Villette, I. Vilfan, and A. Bourret, Phys. Rev. Lett. **73**, 1825 (1994).
[9] E. A. A. Jarvis and E. A. Carter, J. Phys. Chem. B **105**, 4045 (2001).
[10] J. V. Lauritsen, M. C. R. Jensen, K. Venkataramani, B. Hinnemann, S. Helveg, B. S. Clausen, and F. Besenbacher, Phys. Rev. Lett. **103**, 076103 (2009).
[11] P. Guénard, G. Renaud, A. Barbier, and M. Gautier-Soyer, Surf. Rev. Lett. **5**, 321 (1998).
[12] J. Ahn and J. W. Rabalais, Surf. Sci. **388**, 121 (1997).
[13] T. Suzuki, S. Hishita, K. Oyoshi, and R. Souda, Surf. Sci. **437**, 289 (1999).
[14] J. Toofan and P. R. Watson, Surf. Sci. **401**, 162 (1998).
[15] E. A. Soares, M. A. Van Hove, C. F. Walters, and K. F. McCarty, Phys. Rev. B **65**, 195405 (2002).
[16] M. Causa, R. Dovesi, C. Pisani, and C. Roetti, Surf. Sci. **215**, 259 (1989).
[17] J. Guo, D. E. Ellis, and D. J. Lam, Phys. Rev. B **45**, 13647 (1992).
[18] I. Manassidis, A. De Vita, and M. J. Gillan, Surf. Sci. Lett. **285**, L517 (1993).
[19] T. J. Godin and J. P. LaFemina, Phys. Rev. B **49**, 7691 (1994).
[20] I. Manassidis and M. J. Gillan, J. Am. Ceram. Soc. **77**, 335 (1994).
[21] V. E. Puchin, J. D. Gale, A. L. Shluger, E. A. Kotomin, J. Günster, M. Brause, and V. Kempter, Surf. Sci. **370**, 190 (1997).
[22] C. Verdozzi, D. R. Jennison, P. A. Schultz, and M. P. Sears, Phys. Rev. Lett. **82**, 799 (1999).
[23] R. Di Felice and J. E. Northrup, Phys. Rev. B **60**, R16287 (1999).
[24] X.-G. Wang, A. Chaka, and M. Scheffler, Phys. Rev. Lett. **84**, 3650 (2000).
[25] R. Baxter, P. Reinhardt, N. López, and F. Illas, Surf. Sci. **445**, 448 (2000).
[26] A. Wander, B. Searle, and N. M. Harrison, Surf. Sci. **458**, 25 (2000).
[27] J. R. B. Gomes, I. de P. R. Moreira, P. Reinhardt, A. Wander, B. G. Searle, N. M. Harrison, and F. Illas, Chem. Phys. Lett. **341**, 412 (2001).
[28] C. Ruberto, Y. Yourdshahyan, and B. I. Lundqvist, Phys. Rev. B **67**, 195412 (2003).
[29] A. Marmier and S. C. Parker, Phys. Rev. B **69**, 115409 (2004).
[30] E. Wallin, J. M. Andersson, E. P. Münger, V. Chirita, and U. Helmersson, Phys. Rev. B **74**, 125409 (2006).
[31] B. Hinnemann and E. A. Carter, J. Phys. Chem. C **111**, 7105 (2007).
[32] G. Kresse, M. Schmid, E. Napetschnig, M. Shishkin, L. Köhler, and P. Varga, Science **308**, 1440 (2005).
[33] M. Schmid, M. Shishkin, G. Kresse, E. Napetschnig, P. Varga, M. Kulawik, N. Nilius, H.-P. Rust, and H.-J. Freund, Phys. Rev. Lett. **97**, 046101 (2006).
[34] M. A. Schildbach and A. V. Hamza, Surf. Sci. **282**, 306 (1993).
[35] T. P. Trainor, P. J. Eng, G. E. Brown, Jr., I. K. Robinson, and M. De Santis, Surf. Sci. **496**, 238 (2002).
[36] A. Christensen and E. A. Carter, Phys. Rev. B **62**, 16968 (2000).
[37] T. Hsu and Y. Kim, Surf. Sci. Lett. **243**, L63 (1991).
[38] M. A. Schildbach and A. V. Hamza, Phys. Rev. B **45**, 6197 (1992).
[39] Th. Becker, A. Birkner, G. Witte, and Ch. Wöll, Phys. Rev. B **65**, 115401 (2002).
[40] P. Hohenberg and W. Kohn, Phys. Rev. **136**, B864 (1964).
[41] M. Levy, Proc. Natl. Acad. Sci. U.S.A. **76**, 6062 (1979).
[42] J. P. Perdew, K. Burke, and M. Ernzerhof, Phys. Rev. Lett. **77**, 3865 (1996).
[43] D. R. Hamann, M. Schlüter, and C. Chiang, Phys. Rev. Lett. **43**, 1494 (1979).
[44] G. B. Bachelet, D. R. Hamann, and M. Schlüter, Phys. Rev. B **26**, 4199 (1982).
[45] N. Troullier and J. L. Martins, Phys. Rev. B **43**, 1993 (1991).
[46] D. Vanderbilt, Phys. Rev. B **41**, 7892 (1990).
[47] W. Kohn and L. J. Sham, Phys. Rev. **140**, A1133 (1965).
[48] Tokyo *ab initio* program package (TAPP) has been developed by a consortium initiated at The University of Tokyo.
[49] O. Sugino and A. Oshiyama, Phys. Rev. Lett. **68**, 1858 (1992).
[50] J. Yamauchi, M. Tsukada, S. Watanabe, and O. Sugino, Phys. Rev. B **54**, 5586 (1996).
[51] H. Kageshima and K. Shiraishi, Phys. Rev. B **56**, 14985 (1997).
[52] T. Kurita, S. Okada, and A. Oshiyama, Phys. Rev. B **75**, 205424 (2007).
[53] R. H. French, J. Am. Ceram. Soc. **73**, 477 (1990).
[54] D. R. Stull and H. Prophet, *JANAF Thermochemical Tables*, 2nd ed. (U.S. National Bureau of Standardism, Washington, DC, 1971).
[55] J.-H. Choi, D.-Y. Kim, B. J. Hockey, S. M. Wiederhorn, C. A. Handwerker, J. E. Blendell, W. C. Carter, and A. R. Roosen, J. Am. Ceram. Soc. **80**, 62 (1997).
[56] M. Gautier, J. P. Duraud, L. P. Van, and M. J. Guittet, Surf. Sci. **250**, 71 (1991).
[57] P. W. Tasker, J. Phys. C **12**, 4977 (1979).
[58] *CRC Handbook of Chemistry and Physics*, edited by D. R. Lide, 85th ed. (CRC Press LLC, Cleveland, 2004).